6226 *Macromolecules* **1998,** *31,* 6226−6233

Light-Scattering Studies of Concentrated Copolymer Micellar Solutions

Yingchun Liu,[†] Sow-Hsin Chen,[‡] and John S. Huang*,[§]

Department of Materials Science and Engineering, Department of Nuclear Engineering, 24-209,
Massachusetts Institute of Technology, Cambridge, Massachusetts, 02139,
and Exxon Research and Engineering Company, Annandale, New Jersey 08801

Received April 30, 1998; Revised Manuscript Received June 29, 1998

ABSTRACT: We report the analyses of an extensive set of light scattering intensity distributions from triblock copolymer micelles in aqueous solutions. We investigated two Pluronics, P84 (PEO$_{19}$-PPO$_{43}$-PEO$_{19}$) and P104 (PEO$_{27}$-PPO$_{61}$-PEO$_{27}$) in an entire range of the disordered micellar phase. Our previous small-angle neutron scattering (SANS) study showed that the micelle is spherical and consists of a compact hydrophobic core and a hydrophilic corona region. In that paper (Liu, Y. C., et al. *Macromolecules* **1998**, *31*, 2236−2244), we proposed a "cap-and-gown" model for the microstructure of the micelle, taking into consideration the polymer segmental distribution and water penetration profile in the core and corona regions. We took into account the intermicellar correlation using the adhesive hard-sphere model of Baxter. With this combined model, we obtained consistent trends for important parameters such as the aggregation number, hydration number per polymer in both the core and corona, and surface stickiness. The structure of the micelle stays essentially constant as a function of concentration, but changes rapidly with temperature. In this paper, we propose a new method for data treatment of static light scattering (LS) intensities at all concentrations which is complementary to the SANS technique. This analysis allows us to extract the average aggregation number of polymer chains in a micelle, the average hydrated volume fraction of a micelle, and the volume fraction of polymers in a micelle. These parameters obtained from SANS and LS agree to within experimental error.

1. Introduction to Pluronics

The triblock copolymers we studied are commercially available under the trade name Pluronic from BASF.[2] They are ABA type block copolymers where the end-symmetric A blocks are poly(ethylene oxide)s and the center B block is polypropylene oxides. These copolymer surfactants are water soluble to large weight percentages and a broad range of temperatures. Pluronic polymer surfactants find widespread industrial use in detergency, foaming/defoaming, emulsification, lubrication, and solublization. They are also used in cosmetics, bioprocessing, and pharmaceutical applications.[2−4]

We focus our attention on a particular Pluronic surfactant family, i.e., copolymers containing 40−60 volume ratio of poly(ethylene oxide)s and polypropylene oxide (see Table 1). This Pluronic family has several members, namely, P104, P94, P84, L64, and L44, with decreasing molecular weights. They can all self-associate into mesoscopic structures in aqueous solutions. Pluronic P104 and P84, with corresponding chemical formulas PEO$_{27}$-PPO$_{61}$-PEO$_{27}$ and PEO$_{19}$-PPO$_{43}$-PEO$_{19}$ are studied in detail. P84 and P104 have molecular weights of 4200 and 5900 DT and molecular volumes of 6920 and 9710 Å^3, respectively. The cloud points of their aqueous solutions are respectively 75 and 85 °C, showing little concentration dependence.

One of the most interesting features of the Pluronic polymer is its self-association in aqueous solution and its resultant rich phase behavior.[3,5−12] At low polymer concentrations and low temperatures, the triblock copolymer in water appear to be single-coils, called unimers. At higher concentrations or temperatures, the copolymer molecules self-associate to form thermodynamically stable micellar aggregates. The micelles exist in a disordered phase within wide temperature and concentration ranges. At even higher concentrations and temperatures, the copolymer chains and micelles can form ordered phases, such as cubic, hexagonal, and lamellar phases.[5,11,12] The self-assembly and phase behaviors of the copolymer solution depends on the total molecular weight and on the composition of the copolymer.

Table 1. Molecular Weights and Molecular Volumes of the Polymer Surfactants of Interest and the Solvent

			molecular volume (Å^3)		
unit	chemical formula	molecular weight (DT)		EO blocks (Å^3)	PO blocks (Å^3)
EO	$-(CH_2)_2O-$	44	72.4		
PO	$-(CH_2)_3O-$	58	95.4		
solvent	D_2O	20	30.3		
P104	PEO$_{27}$-PPO$_{61}$-PEO$_{27}$	5900	9729	3910	5819
P84	PEO$_{19}$-PPO$_{43}$-PEO$_{19}$	4200	6853	2751	4102
L44	PEO$_{10}$-PPO$_{23}$-PEO$_{10}$	2200	3642	1448	2194

Micellization occurs above a certain critical micellization concentration and temperature (cmc and cmt). The cmc and cmt curves of the Pluronic surfactants have been studied extensively using various techniques.[6a,7,13,14] Dynamic light scattering shows that Pluronic micellar solutions exhibit significant polydispersity at low temperatures but become monodisperse at high temperatures.[6a,b] Batch-to-batch of the surfactant supplied contains composition heterogeneities, such as diblock copolymer impurities. This may considerably affect micelle formation and surface tension but have little effect on the micellar structure and intermicellar interaction for concentrations and temperatures beyond the cmc−cmt lines. We focus attention on the microstruc-

---

[†] Department of Materials Science and Engineering, Massachusetts Institute of Technology.

[‡] Department of Nuclear Engineering, Massachusetts Institute of Technology.

[§] Exxon Research and Engineering Co.

S0024-9297(98)00695-0 CCC: $15.00

ture and interaction of micelles far beyond micellization boundaries and ignore such impurities and heterogeneities. The experimental cmc−cmt boundaries of the Pluronic P104, P84, and L44 in aqueous solutions are determined using scattering methods.[15] Micelles are formed as temperature or concentration increase beyond the cmc−cmt curves. One observes an abrupt increase of the scattering signals when crossing cmc−cmt lines.

Gelation of Pluronic solutions occurs at high polymer concentrations. For the 40% EO Pluronic family, concentration of the sol−gel transition is only slightly dependent on temperature. The sol−gel boundary is nearly vertical on the phase diagram. For stable micellar solutions at temperatures higher than 30 °C, the variation of gelation concentration is normally about 1 or 2 wt % within a large temperature range. The gelation concentrations for Pluronic P104, P84, and L44 are 20, 22, and 24 wt %, respectively. These gelation concentrations set the limit for the concentration ranges of the disordered micellar phases. At about 20 wt %, when the hydration effect of the copolymer is taken into account, the volume fraction of the micelles in solution can be as high as 40−50%. Since the thermodynamic properties of the solution depend on the hydrated volume fraction rather than that of the dry one, it is expedient to find a convenient method in the laboratory to measure this quantity without having to invoke the SANS method, which is not always assessable.

In this paper, a novel light scattering intensity analysis method is developed which is valid up to about 50% volume fraction. The new light scattering intensity analysis method significantly extends the concentration range of the traditional Zimm plot.[16] Its simplicity makes it useful also as a fingerprint to detect phase transitions.

2. Static Light Scattering Measurements

Light-scattering experiments were performed at the Corporate Research Laboratories, Exxon Research and Engineering Co. A standard Brookhaven Instrument photon correlator was used for the measurements of both static and dynamic light scattering of the Pluronic solutions. The light scattering apparatus uses a He−Ne laser, of wavelength 632.8 nm at a power level of 15 mW, mounted on a goniometer covering an angular range of 25°−135°. A Pyrex glass sample cell was positioned at the center of a brass thermostat block. The temperature of the sample was controlled by a Brookfield water bath with an accuracy of 0.1 °C. The index-matching fluid surrounding the cell was filtered toluene.

Two major calibrations were performed for the light-scattering apparatus.

(i) Angular Scattering Envelope. The optics were calibrated to ensure a symmetrical envelope for different scattering angles. For angular calibration we used a standard solution of polystyrene latex 18 nm in diameter. The standard solution was filtered right before the calibration in order to remove any possible large aggregates during storage.

(ii) Absolute Scattering Cross Section. For each slit in front of the photo detector, intensity calibration was performed with toluene of known Rayleigh scattering cross section per unit volume ($R_{\text{toluene}} = 1.406 \times 10^{-5}$ cm^{-1}). The calibration constant was thus determined experimentally in order to convert the photodetector count rate into an absolute scattering intensity, which is the Rayleigh ratio.

Table 2. Refractive Index Increment for Pluronic P104 Polymer at High Concentrations in Water[a]

concn C (g cm^{-3})	Δn[a]			
	25 °C	35 °C	45 °C	55 °C
0.0300	0.003966	0.003793	0.003714	0.003643
0.0500	0.006536	0.006275	0.006153	0.006038
0.0783	0.009743	0.009418	0.009218	0.009045
0.0980	0.01295	0.01255	0.01229	0.01206
0.1380	0.01856	0.01793	0.01756	0.01723
0.1900	0.02516	0.02472	0.02421	0.02375

[a] The refractive index increment ($\Delta n = n - n_0$, where n_0 is refractive index of the solvent) shows linear dependence on concentration increment, Δc.

Table 3. Refractive Index Increment dn/dc [g^{-1} cm^3] for P104, P84, and L44 at Various Temperatures

	25 °C	35 °C	45 °C	55 °C
P104	0.1342	0.1321	0.1293	0.1269
L44	0.1341	0.1316	0.1297	0.1243
P84	0.134		0.129	

Pluronic polymers were dissolved in deionized, filtered water at various concentrations. The solutions were contained in Pyrex glass vials with thermoset plastic caps. Refrigeration was helpful to dissolve the polymers, especially at high concentrations. The samples were stored at room temperature for a few days for stabilization before filtration. About 5 mL of each sample was then extracted and filtered with a 0.22 μm filter unit individually. All light-scattering measurements were performed at least 1 h after the filtration to ensure completed aggregation equilibrium.

Characterization of a polymer solution with static light scattering requires measurement of the refractive index increment of the solution as function of polymer concentration. Strictly speaking, for a system with compositional heterogeneity, the apparent molecular weight M and the weight-average molecular weight M_W are related by[17]

$$M\left(\frac{\mathrm{d}n}{\mathrm{d}c}\right)^2 = M_w\left(\frac{\mathrm{d}n}{\mathrm{d}c}\right)_A\left(\frac{\mathrm{d}n}{\mathrm{d}c}\right)_B + \left[\left(\frac{\mathrm{d}n}{\mathrm{d}c}\right)_A^2 - \left(\frac{\mathrm{d}n}{\mathrm{d}c}\right)_A\left(\frac{\mathrm{d}n}{\mathrm{d}c}\right)_B\right] w_A M_{WA} + \left[\left(\frac{\mathrm{d}n}{\mathrm{d}c}\right)_B^2 - \left(\frac{\mathrm{d}n}{\mathrm{d}c}\right)_A\left(\frac{\mathrm{d}n}{\mathrm{d}c}\right)_B\right] w_B M_{WB}$$

where M_{WA} and M_{WB} are the weight-average molecular weights of component A and B, and w_A and w_B are the weight fractions of A and B, respectively. For Pluronic copolymers, the two components PEO and PPO have very close refractive indices. The apparent molecular weight and the weight-average molecular weight are therefore not distinguished in this work.

The refractive index increments dn/dc (Tables 2 and 3) for Pluronic polymer in water were measured using a differential refractometer at temperatures ranging from 25 to 60 °C. The refractometer was equipped with a built-in laser unit of the same wavelength as the scattering apparatus ($\lambda = 632.8$ nm), and temperature was controlled with an accuracy of 1 °C. The refractive index increments for concentrated solutions were measured using a series of reference of the same polymer solution of various concentrations. The actual values of refractive index dn/dc were obtained through a calibration constant.

The refractive index increment, $\Delta n = n - n_0$, where n_0 is the refractive index of the solvent, shows linear dependence on concentration increment, $\Delta\chi$.

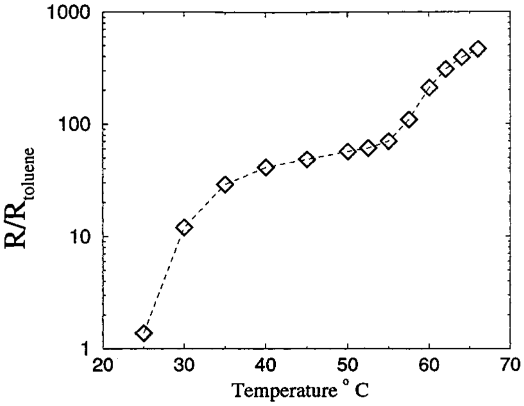

Figure 1. Light-scattering intensity of 3% Pluronic P84 solutions from 20 to 66 °C. The intensity indicates the evolution of structures from unimer to micelle and to bigger aggregates as temperature increases.

For Pluronic polymer concentrations from dilute up to 20 wt %, the refractive index increments were measured as a function of temperature and concentration. It is found that d*n*/d*c* does not depend on the polymer concentration. However, it has a weak temperature dependence. The refractive index decreases at higher temperatures. In the temperature range considered in our measurements, the refractive index of Pluronic P104 varies linearly with the temperature. By fitting the refractive index at four temperatures, 25, 35, 45, and 55 °C, an empirical linear relation is obtained as $dn/dc = 0.1405 - 0.0002461T$ [g^{-1} cm^3], where T is the temperature in centigrade. This linear relationship holds at each concentration of polymer. No molecular weight dependence is observed. The constants of refractive indices are used to calculate the absolute light scattering intensity of the polymeric micellar solutions at various temperatures.

The corrected scattering intensity showed no angular dependence because the nanometer size of a micelle is much smaller compared with the wavelength of light. The measurements were made at a fixed scattering angle of 90°. Commercial software (BI9K) from Brookhaven Instrument was used to measure the dynamic light scattering. The static scattering intensity was given simultaneously.

A typical scattering intensity measured at $\theta = 90$ ° (normalized by scattering from toluene) for a 3% P84 solution as a function of temperature is shown in Figure 1. The amplitude of the intensity reflects the crossing of various phases as the temperature increases. The weak scattering at low temperatures indicates the presence of unimers. At 30 °C, the intensity starts rising, indicating the formation of larger aggregate, micelles. The intensity increases slowly with temperature until about 55 °C, signifying a gradual increase in micellar molecular weight. An abrupt increase in intensity at 55 °C indicates onset of formation of even larger structures. Beyond 60 °C, the scattering intensity shows apparent angular dependence, indicating the formation of submicron and micron sized aggregates.

The goal of our experiments is to study light scattering from concentrated micellar solutions. Light scattering from Pluronic P104, P84, and L44 was measured from room temperature to 55 °C. For each temperature, we plot the scattering intensity against the polymer concentration. Three regions are present in a typical plot over the entire concentration range. The scattering intensity increases with concentration at low concentrations, reaches a broad plateau at intermediate concentrations, and decreases with concentration at high concentrations. The overall intensity increases with temperature. The peak positions slightly shift with temperature. Figures 2 and 3 show the light scattering from P104 and P84 solutions, respectively, as a function of the polymer concentration at a given temperature (dashed lines are to guide the eyes). The peaks shift to lower concentration and higher amplitude at higher temperatures.

Our central task is to interpret the static scattering intensity quantitatively. The three regions demonstrate the characteristic colloidal behaviors of the polymeric micellar solutions. The initial increase with concentration is easily understood as due to the increase of the number densities of the scatters. The decease with concentration at the high concentrations is a consequence of the interparticle interactions. The peak in the intermediate concentration region is a result of the two competing effects.

The amplitude and shape of the scattering intensity vs concentration curve contain information on the average micellar molecular weight, volume fraction, and an interaction parameter. A systematic method is needed to extract these important parameters explicitly from the scattering data. We shall develop such a method and apply it to the polymeric micellar solutions in subsequent sections.

3. Static Light Scattering Analysis

The classical procedure of polymer characterization using static light scattering involves extrapolation of the scattered light intensity (excess Rayleigh scattering) to the zero concentration limit. In the dilute limit, the product of the inverse light scattering cross-section per unit volume (Rayleigh ratio) and concentration is a linear function of the concentration. The two coefficients in the linear equation are the weight average molecular weight and a quantity proportional to the second viral coefficient, $B_2 = N_A m^2 A_2$, of the solution, where N_A is the Avogadro's number and m the mass of the particle. The well-known Zimm plot, when applied to a micellar solution, uses the following formula[16]

$$\frac{KC}{R_\theta} = \frac{1}{M\bar{P}(k)} + 2A_2C \qquad (1)$$

where $C = c - \text{cmc}$ (c and cmc are the polymer concentration and critical micellization concentration in units of grams of solute per milliliter), M is the weight average molecular weight of the micelle in (g/mol), A_2 is the quantity proportional to the second viral coefficient B_2 in units of (mL mol/g^2), and R_θ is the excess Rayleigh ratio in unit of cm^{-1}. When the particle size is comparable with the wavelength of light, a normalized particle structure factor $\bar{P}(k)$ is needed. It is often simplified as $1 - (R_g k)^2/3$ where R_g is the radius of gyration of the micelle and $k = (4\pi/\lambda_0)n_0 \sin(\theta/2)$, the magnitude of the scattering wave vector in the solvent. The optical constant K is defined as $K = 4\pi^2 n_0^2 (dn/dc)^2/N_A\lambda_0^4$, where n_0 is the refractive index of water and λ_0 the laser wavelength in air. The essential quantity is C/R_θ. The plot of C/R_θ vs C deviates from linearity significantly at higher concentrations. Several data points in the low-concentration region may be selected and extrapolated to zero concentration. However this

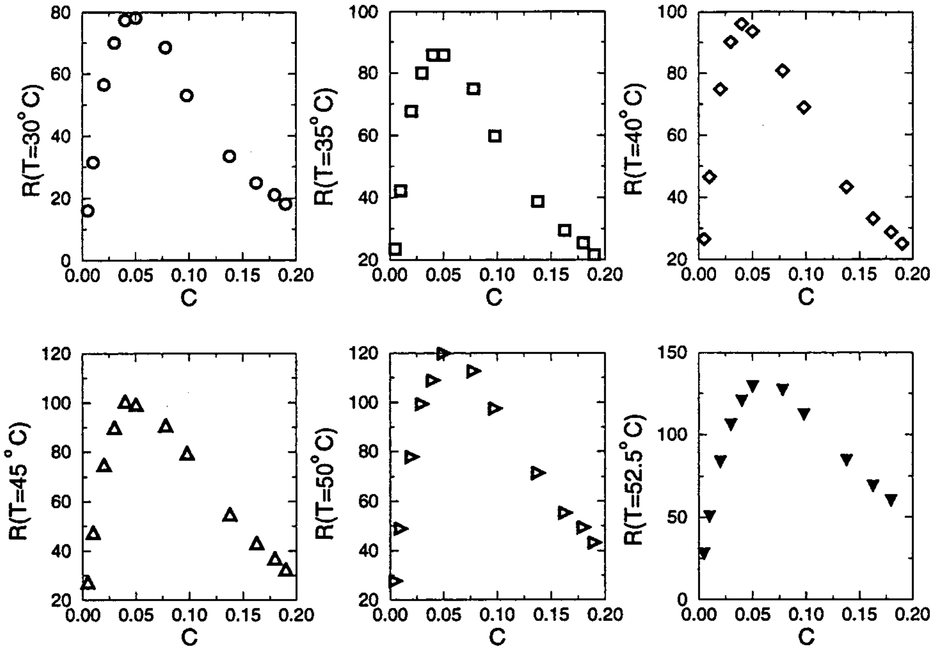

Figure 2. Light-scattering intensities of Pluronic P104 solutions as a function of concentration (in wt %) at temperatures from 30 °C to 52.5 °C.

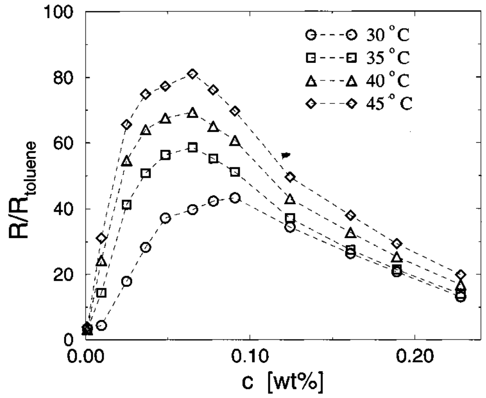

Figure 3. Light-scattering intensities of Pluronic P84 solutions as a function of concentration (in wt %) at temperatures from 30 °C to 45 °C.

approach is somewhat ambiguous for treatment of data from polymeric micelles. First, there are few experimental data points in the low-concentration region in practice. A slight variation in the choice of concentration range can result in a large difference in the slope and intercept of the Zimm Plot. Second, a slight uncertainty in the background subtraction can result in a large error in the inverse Rayleigh ratio due to the relatively small signal-to-noise ratio. This problem is particularly severe for polymeric micellar solutions because of the inaccuracy in determination of the background scattering from unknown impurities and heterogeneity's and from the unimers. For these reasons, the traditional zero-concentration extrapolation method is not appropriate for polymeric micellar solutions. A better treatment needs to take advantage of the data at higher concentrations, where scattering signals are stronger and less affected by the background. Proper consideration for the interparticle correlation in terms of the structure factor is essential in the theoretical formulation of static light scattering intensity for a broad concentration range.

The Rayleigh ratio can be written in terms of the normalized particle structure factor $\bar{P}(k)$ and the interparticle structure factor $S(k)$ as

$$R_\theta = KCM\bar{P}(k)S(k) \tag{2}$$

In the case of polymeric micelles having diameters in the range of 10−20 nm, the zero k limit can be taken safely (i.e. $\bar{P}(k) = 1$). The Rayleigh ratio can then be written as $R_\theta = KCMS(0)$. Thus for high concentrations,

$$\frac{KC}{R_\theta} = \frac{1}{M}\frac{1}{S(0)} \tag{3}$$

The traditional method of viral expansion can be considered as an expansion of $1/S(0)$ to the first order in concentration. The structure factor at zero wave vector transfer $S(0)$ is a thermodynamic quantity that can be obtained from the equation of state and is proportional to the osmotic compressibility of the solution.

4. A New Method for Light Scattering Intensity Analysis

A new plot is proposed which treats the light scattering intensity from zero to high concentrations on equal footing. Analogous to the well-known Zimm plot, the central quantity is KC/R_θ. It is based on an observation that a plot of $\ln(KC/R_\theta)$ vs C yields approximately a straight line in the entire concentration range, up to volume fractions of about 50%. We rewrite the previous equation as,

$$\ln\left[\frac{KC}{R_\theta}\right] = -\ln(M) + \ln\left[\frac{1}{S(0)}\right] \tag{4}$$

The slope of the new plot, which is derived from the concentration expansion of logarithm of the inverse structure factor, contains information on osmotic compressibility as a result of interparticle interactions. Analogous to the traditional plots, the zero intercept gives the weight-average molecular weight of the micelle. The logarithm of $1/S(0)$ has nearly linear rela-

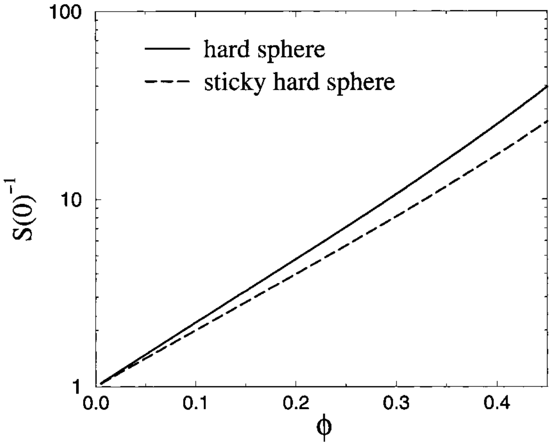

Figure 4. Logarithm of $1/S(0)$ for hard spheres and sticky hard spheres exhibits almost linear dependence on volume fraction ϕ.

tionships with the volume fraction for both hard sphere and sticky hard sphere systems, as illustrated in Figure 4. The slope of $\ln(1/S(0))$ for the hard sphere system is 8. The difference between $1/S(0)$ and $\exp(8\phi)$ is less than 4%. On the logarithmic scale, the differences between $\ln(1/S(0))$ and 8ϕ is at most 2% for the volume fraction range from 0 to 0.45. This level of difference is usually within experimental error. To the first approximation, the new plot can be adopted as a simple way of obtaining the volume fraction from the slope. The linear shape of the new plot holds also for a sticky hard sphere system. In the sticky hard sphere model, the slope is $8 - 2/\tau$. As stickiness increases, the slope gets smaller. This new plot can be an easy and intuitive way of extracting useful parameters. It becomes extremely straightforward if the association and interactions are independent of polymer concentration. The self-assembling polymeric micelles is exactly such a case.

To see the plausibility of these statements, we can express the structure factor at $k = 0$ of a hard sphere system in terms of the Carnahan–Stirling equation of states[18] as

$$\frac{1}{S(0)} = \frac{1 + 4\phi + 4\phi^2 - 4\phi^3 + \phi^4}{(1 - \phi)^4} = 1 + 8\phi + 30\phi^2 + 72\phi^3 + 140\phi^4 + ... \quad (5)$$

In comparison, the expansion of the exponential functions is $\exp(8\phi) = 1 + 8\phi + 32\phi^2 + (256/3)\phi^3 + ...$, which quite closely approximates the above expansion for a sticky hard sphere system,[19,20] the corresponding expansion is

$$1/S(0) = 1 + (8 - 2/\tau)\phi + \frac{18\tau + 192\tau^3 - 90\tau^2 - 1}{6\tau^3}\phi^2 ... \quad (6)$$

In the case of hard sphere potential, the second virial coefficient of $1/S(0)$ is 8. For the sticky hard spheres having potential in the Baxter form,[19,20] it is $8 - 2/\tau$. Higher order expansion terms in ϕ result approximately in an exponential function. In each case, the function $\ln(1/S(0))$ has a maximum deviation from 8ϕ or $(8 - 2/\tau)\phi$ of about 2%. The simplicity of this relationship may stimulate further experimental studies of systems with a variety of interaction potentials such as short- and long-range ionic repulsions.

5. Applications of the New Plot

The new plot takes advantage of larger scattering signals from concentrated solutions and overcomes the difficulties in extrapolating to zero concentration. It has obvious advantages over the traditional analysis methods which require frequent and tedious instrument calibrations and background measurements due to weak scattering signals from dilute solutions. Estimation of the background scattering can often be particularly ambiguous for a system displaying complex association behaviors at low concentrations. An analysis that deals with signals having a large signal-to-noise ratio can drastically reduce the uncertainty caused by errors in background subtraction. The most useful feature of the new plot is its near linearity within a broad range of volume fractions. Any significant deviation from linearity can be considered a fingerprint of a phase transition. This feature provides a quick and intuitive way to detect possible phase transitions by static light scattering from a series of solutions.

The new plot extends the working range of static light scattering up to about 50% of volume fraction, equivalent to 10–100 times the concentration range used in the classical treatment. We plot $\ln(KC/R)$ vs C. The plot will be very closely linear. The intercept of the line with the ordinate gives the logarithm of the inverse molecular weight of the micelle or the aggregation number. The slope of the line contains information on the hydrated volume fraction, a quantity difficult to obtain with other light scattering techniques.

The slope of this plot yields effectively the volume fraction of the polymers in a micelle. The slope is $(8 - 2/\tau)\phi/C$. According to values of the molecular volumes of D_2O, EO, and PO groups listed in Table 1, densities of both the polymers and the solvent are effectively 1.0 to within 1%. The slope can now be expressed as the volume ratio of the bound solvent molecules to the polymer in a micelle, i.e.

$$\text{slope} = \left(8 - \frac{2}{\tau}\right)\left(1 + \frac{V_{\text{solvent}}}{V_{\text{polymer}}}\right) \quad (7)$$

When the excluded volume repulsion dominates, $2/\tau \ll 8$ (τ is of the order of 5), the volume ratio of bound water molecules can immediately be estimated from the slope,

$$\text{slope} = 8\left(1 + \frac{V_{\text{solvent}}}{V_{\text{polymer}}}\right) \quad (8)$$

Alternatively, the slope can be related to an important parameter of the polymeric micellar solutions, namely, the overall polymer volume fraction in a micelle, ϕ_{polymer}, which is given by $V_{\text{polymer}}/(V_{\text{polymer}} + V_{\text{solvent}})$. The number of bound-solvent molecules per polymer chain can then be calculated. This new plot gives a convenient way to evaluate the solvation and overall polymer volume fraction in a micelle from static light scattering intensity taken at 90° at a series of polymer concentrations.

6. Analysis of Light Scattering from Pluronic Micellar Solutions

Static light scattering intensities from Pluronic micellar solutions are processed using the new plot. The working concentration range is extended to the maximum volume fraction of the disordered micellar phase. It is especially useful for micellar solutions exhibiting complicated phases in the dilute solutions.

Strictly speaking, micelle formation is not a phase-transition process but a gradual transition having a region with a coexistence of unimers and micelles. The scattering intensity as a function of concentration within the mixed phase near the cmc is very complex and usually not explicitly defined. However, at concentrations a few times of the cmc, scattering from the unimers can be considered a background. The cross term of the unimer−micelle scattering is usually ignored. The scattering intensity is then mainly due to the scattering from micelles. The complexity is overcome by using the strong scattering from larger concentrations.

To characterize the polymeric micellar solutions, the new plot can be used to analyze light scattering data from a group of samples having low to high polymer concentrations at a given temperature. We have already known from SANS analyses that the microstructure of the micelle is independent of the polymer concentration at a given temperature.[1] This feature of the Pluronic micelles is an important starting point of our light scattering analyses.

In the following, the *x*-axis and *y*-axis of the plot are the polymer concentration *C* in weight percentage and logarithm of *CK*/*R*, respectively. The zero intercept of the plot gives ln(1/*M*). The slope of the plot contains the information on the interparticle interaction and solvation. As an example, a new plot of a scattering intensity normalized by toluene scattering is shown in Figure 5 for a series of Pluronic P104 micellar solutions at 45 °C.

Light-scattering data have been analyzed using the new plot for Pluronic P104, P84, and L44 solutions at various temperatures. Results of the analysis for Pluronic P104, P84, and L44 micellar solutions are listed in Tables 4−6. A linear relationship in ln(*C*/*R*) against *C* holds for all the micellar solutions considered. The plots are shown in Figures 6 and 7

At moderate temperature (30−45 °C), the slopes are 20.2 for Pluronic P104 (M_W = 5900), 17.5 for Pluronic P84 (M_W = 4200), and 12 for Pluronic L44 (M_W = 2200). These values indicate that the volume ratios of the hydrated water molecules to the polymer chains are 2.5, 2.1, and 1.5 for Pluronic P104, P84, and L44, respectively. This means that the overall polymer volume fractions in a micelle are about 40%, 50%, and 70% for Pluronic P104, P84, and L44 block copolymer surfactants. The trend of the ratios clearly indicates that the ability to carry solvent molecules increases with the molecular weight of the polymer surfactant.

The effect of polymer molecular weight on micelle structure for a given copolymer composition is clear. For example, new plots for P104 at 40 °C, P84 at 40 °C, and L44 at 55 °C show that the total molecular weights of the micelles obtained from the intercepts are 489, 222, and 90 kDa, corresponding to the aggregation numbers of 82, 53, and 41, for P104, P84, and L44, respectively. We note that at low temperatures when SANS analysis fails, LS still gives a reasonable estimation of aggregation number and hydration number. Compared with SANS, the LS technique seems to tolerate more of the complexity. Analysis of LS intensities is also much simpler.

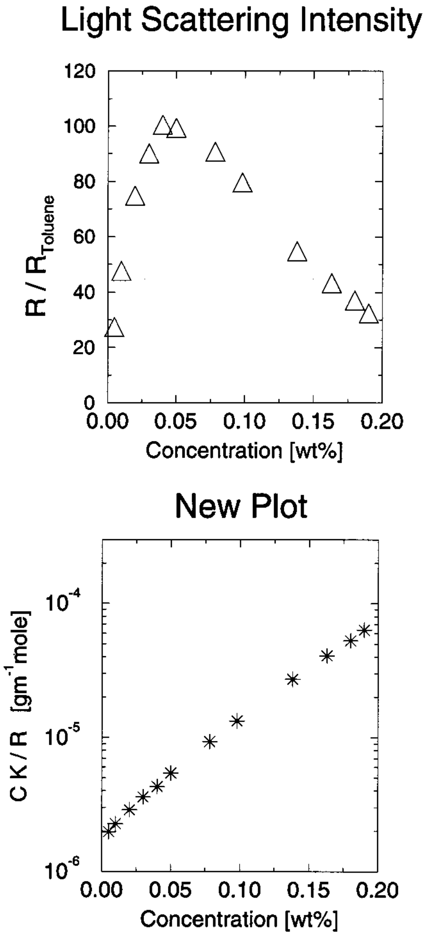

Figure 5. Light-scattering intensities of P104 micellar solutions at 45 °C as function of their concentrations plotted in linear scales and the analysis in terms of the new plot.

Table 4. Characterization of Light Scattering from Pluronic P104 Micellar Solutions Using the New Plot

T (°C)	slope, (8 − 2/*τ*)*ϕ*/*C*	molecular weight (10^6)	aggregation no., *N*
30	20.4	0.373	64
35	20.2	0.434	74
40	20.0	0.489	82
45	18.5	0.499	85
50	17.1	0.527	89
52.5	16.1	0.555	94
55	15.8	0.576	98

Table 5. Characterization of Pluronic P84 Micellar Solutions Using the New Plot

T (°C)	slope, (8 − 2/*τ*)*ϕ*/*C*	molecular weight (10^6)	aggregation no., *N*
30	17.9	0.138	33
35	17.6	0.182	43
40	17.4	0.222	53
45	17.0	0.272	65
50	16.8	0.291	69
55	16.4	0.327	78

The total molecular weight of the micelle and the slope can also be calculated from the SANS parameters. Compared with SANS results, the values of micellar molecular weight and hydration number of the micellar solutions obtained from light scattering agree within 10−20%. As an example, micellar parameters deduced from SANS data analysis for P85 are listed in the Table 7 for comparison.

Table 6. Volume Fraction and Molecular Weight and Aggregation Number Obtained from Analysis of Light-Scattering Intensity of Pluronic L44

T (°C)	slope, $(8 - 2/\tau)\phi/C$	molecular weight (10^3)	aggregation no., N
55	12 ± 0.5	90	41
50	12 ± 0.5	67	30
45	12 ± 0.5	39	18

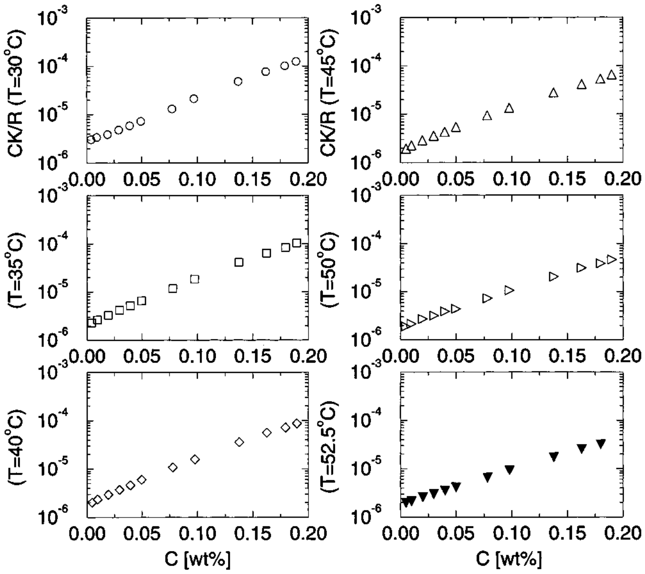

Figure 6. New plots of light-scattering intensities of Pluronic P104 micellar solutions at different temperatures.

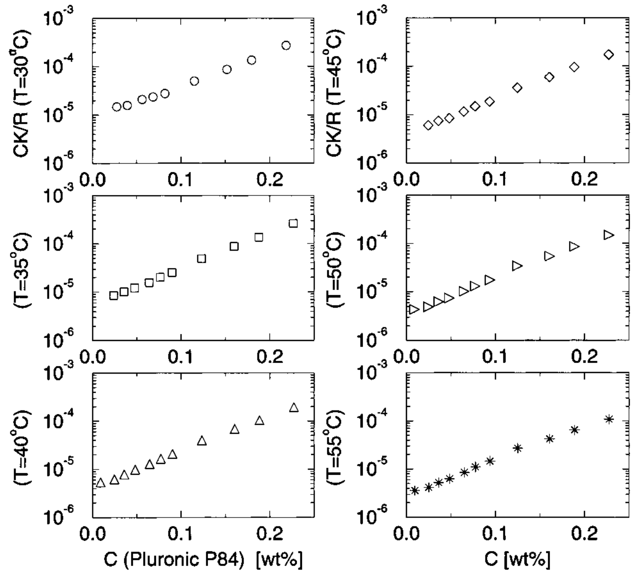

Figure 7. New plots of light-scattering intensities of Pluronic P84 micellar solutions at different temperatures.

Table 7. Parameters of the Microstructure and Interaction for P84 Polymeric Micelles Extracted from SANS Experiments

T (°C)	aggregation no., N	hydration, H	core radius (nm)	diameter (nm)	$\frac{1}{\tau}$
35	44	240	3.7	10.5	0.1
40	54	210	3.8	10.8	0.25
45	66	190	4.0	11.5	0.35
55	80	130	4.3	11.8	0.45

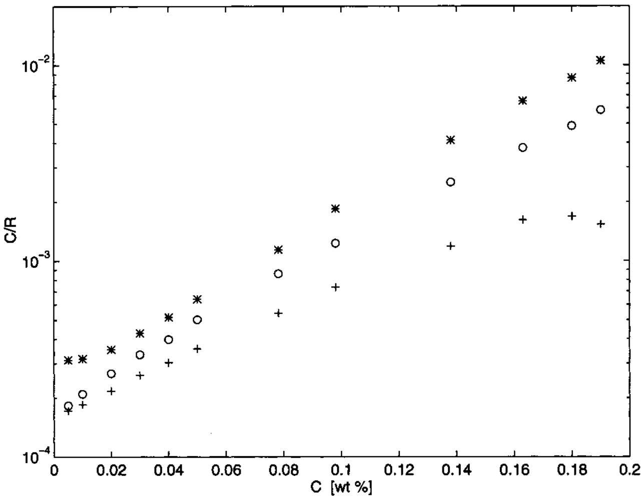

Figure 8. An illustration showing that phase transitions correspond to deviations from a linear shape in the new plot. Light scattering from Pluronic P104 illustrates three cases at 28 °C (∗) (micellization), 45 °C (○), and 55 °C (+) (disorder-to-order transition).

7. Conclusion

In this paper we proposed and demonstrated its utility of a plot for LS intensity which is an extension of the classical Zimm plot to higher concentrations. This new plot is a convenient way of obtaining the weight-average molecular weight and the hydrated volume fraction of a copolymer micelle as a function of temperature when the microstructure of the micelle stays constant as a function of the polymer concentration. It can also be used for detecting the crossing of phase boundaries as the concentration increases at a constant temperature, as shown in Figure 8. This method should be applicable in nonionic colloidal systems at moderate concentration range, as long as the structure and the nature of interactions are independent of concentration.

Acknowledgment. This research is supported by a grant from Materials Sciences Division of the US DOE. The light-scattering experiments were performed at the Exxon Research and Engineering Co., Annandale, NJ, and we appreciated their support.

References and Notes

(1) Liu, Y. C.; Chen, S. H.; Huang, J. S. Small-Angle Neutron Scattering Analysis of the Structure and Interaction of Triblock Copolymer Micelles in Aqueous Solution. *Macromolecules* **1998**, *31*, 2236−2244.

(2) Pluronic and Technical Brochure: Tetronic Surfactants. BASF Corp., Parsipanny, NJ 1989.

(3) Alexandridis, P.; Hatton, T. A. *Colloids Surf.* **1995**, *96*, 1.

(4) Chu, B. *Langmuir* **1995**, *11*, 414.

(5) Wanka, G. Hoffmann, H.; Ulbricht, W. *Macromolecules* **1994**, *27*, 4145.

(6) (a) Zhou, Z.; Chu, B. *J. Colloid Interfacial Sci.* **1988**, *126*, 171. (b) Goldmints, I. F. K. Holtzwarth, J. F.; Smith, K. A.; Hatton, A. *Langmuir* **1997**, *13*, 6130−6134.

(7) Brown, W.; Schillen, K.; Almgren, M.; Hvidt, S.; Bahadur, P. *J. Phys. Chem.* **1991**, *95*, 1850.

(8) Schillen, K. Brown, W.; Johnsen, R. M. *Macromolecules* **1994**, *27*, 4825.

(9) Mortensen, K. *Prog. Colloid Polym. Sci.* **1993**, *91*, 69.

(10) Almgren, M. Alsins, J.; Bahadur, P. *Langmuir* **1991**, *7*, 446.

(11) Almgren, M. Brown, W.; Hvidt, S. *Colloid Polym. Sci.* **1995**, *273*, 2.

(12) Mortensen, K. Brown, W.; Jorgensen, E. *Macromolecules* **1994**, *27*, 5654.

(13) Alexandridis, P.; Athanassiou, V.; Fukuda, S.; Hatton, T. A. *Langmuir* **1994**, *10*, 2604.

(14) Grieser, F.; Drummond, C. J. *J. Phys. Chem.* **1988**, *92*, 5580.

(15) Liu, Y. Microstructure of Micelles Formed by Triblock Copolymer in Water and Relation to Rheology of Solutions. Ph.D. Thesis, MIT, June 1997.
(16) Flory, P. J. *Principles of Polymer Chemistry*. Cornell University Press 1953.
(17) Chu, B. *Light Scattering-Basic Principles and Practice*, 2nd ed.; Academic Press: San Diego, 1991.
(18) Canahan-Stirling, *J. Chem. Phys.* **1969**, *51*, 635.
(19) Baxter, R. J. *J. Chem. Phys.* **1968**, *49*, 2770.
(20) Liu, Y. C.; Chen, S. H.; Huang, J. S. *Phys. Rev. E* **1996**, *54*, 1698.

MA980695C